

SCIENTIFIC DATA

OPEN

DATA DESCRIPTOR

Multiple-data-based monthly geopotential model set LDCmgm90

Wei Chen^{1*}, Jiesi Luo¹, Jim Ray², NanYu³ & Jian Cheng Li¹

While the GRACE (Gravity Recovery and Climate Experiment) satellite mission is of great significance in understanding various branches of Earth sciences, the quality of GRACE monthly products can be unsatisfactory due to strong longitudinal stripe-pattern errors and other flaws. Based on corrected GRACE Mascon (mass concentration) gridded mass transport time series and updated LDCgam (Least Difference Combination global angular momenta) data, we present a new set of monthly gravity models called LDCmgm90, in the form of Stokes coefficients with order and degree both up to 90. The LDCgam inputs are developed by assimilating degree-2 Stokes coefficients from various versions of GRACE (including Mascon products) and SLR (Satellite Laser Ranging) monthly gravity data into combinations of outputs from various global atmospheric, oceanic, and hydrological circulation models, under the constraints of accurately measured Earth orientation parameters in the Least Difference Combination (LDC) scheme. Taking advantages of the relative strengths of the various input solutions, the LDCmgm90 is free of stripes and some other flaws of classical GRACE products.

Background & Summary

Time-dependent gravity from the GRACE (Gravity Recovery and Climate Experiment) twin satellites is of great significance for studies related to changes in land water, ice sheets, sea level rise, ocean circulation, Earthquake dynamics etc.^{1–7}. GRACE data are routinely provided almost every month (from Apr. 2002 to Jun. 2017, but with 20 months missing) in the form of Stokes coefficients with AOD1B (Atmosphere and Ocean Dealiasing Level 1B) corrections (denoted as GSM) by Center for Space Research (CSR), Deutsches GeoForschungsZentrum (GFZ), Jet Propulsion Laboratory (JPL) and Graz University of Technology (TUG), using a least squares adjustment (LSA) scheme^{8–14}. There are often limited agreements between GRACE-based results and those obtained by independent observations, mostly attributed to the well-known strong striped noise patterns caused by the GRACE's near-polar orbital inclination and the LSA scheme, which ignores the orthogonality of spherical harmonics and thus leads to correlations of Stokes coefficients^{15–19}. Notable discrepancies can also be found among GRACE products released by different institutes, due to some differences in data processing strategies adopted by them^{8–13,19–22}. Various filtering and destriping methods are proposed to attenuate these stripes, resulting in weaker and distorted signals of interest^{23–28}. Moreover, power losses are also found around 3 cycles per year (cpy) and higher in time series of low degree GRACE Stokes coefficients²¹.

Since 2015, CSR and JPL also provide so-called Mascon solutions using the Mass Concentration blocks (mascons)^{29–32}, another form of gravity field basis functions. With mascons, some a priori geophysical constraints can be implemented to remove noises from the GRACE observations at the Level-2 processing step, which is a much more rigorous approach than the empirical post-processing filtering and destriping of the LSA-based spherical harmonics. However, the problem of power losses around 3 cpy and higher is not overcome, and notable differences between CSR and JPL mascon solutions still exist (noted by this study).

Mass redistributions will cause changes not only in gravity but also in Earth's pole coordinates and spin rate, due to conservation of angular momentum^{33,34}. Plenty of studies have explored the links between the time-dependent Stokes coefficients and Earth rotational variations, specifically the level of agreement between GRACE-based (C_{21} , S_{21}) series and polar motion, and between SLR-based C_{20} and length-of-day (LOD) variations after contributions unrelated to mass redistributions are excluded^{21,35–45}. Some even made use of these GRACE and/or SLR (Satellite Laser Ranging) coefficient series to improve geophysically based fluid model excitations of polar motion and LOD variations^{21,22,46}. Among these studies, the Least Difference Combination (LDC) of global

¹Collaborative Innovation Center of Geospatial Technology/Key Laboratory of Geospace Environment and Geodesy, School of Geodesy and Geomatics, Wuhan University, Wuhan, China. ²Retired: National Oceanic and Atmospheric Administration, Silver Spring, Maryland, USA. ³College of Marine Science and Technology, China University of Geosciences, Wuhan, China. *email: wchen@sgg.whu.edu.cn

angular momenta for surficial geophysical fluids of Chen *et al.*²¹ and Yu *et al.*²² (hereafter termed as LDCgam) seem to have the best performances in both the frequency and time domains, since various versions (CSR, GFZ and JPL) of GRACE and SLR monthly gravity data (RL05) were assimilated into the outputs from various global atmospheric, oceanic, and hydrological circulation models, in the LDC scheme which can extract the best frequency components from various types of data sources provided that one or more proper reference data or models can be established^{21,47}.

To summarize, the currently available GRACE monthly Stokes coefficients are unsatisfactory due to strong longitudinal stripe-pattern errors and other flaws while assimilating independent related observations may help to improve them. In this study, we used numerical integration to convert Mascon gridded mass to Stokes coefficients and applied necessary corrections as described in the next section. We also prepared for this study an updated LDCgam solution⁴⁸ obtained by similar procedures in Chen *et al.*²¹ and Yu *et al.*²² but assimilating all RL05 and RL06 GRACE/SLR Stokes coefficients from CSR, GFZ, JPL and TUG, and all RL05 and RL06 Mascon gridded mass fields. Then we put forward the improved monthly gravity model set LDCmgm90, in the form of Stokes coefficients (complete from degree and order 2 to 90) since they are more convenient to use.

Methods

The GRACE monthly data are usually released together with the GRACE AOD1B products, which provide a model-based data-set (including GAA, GAB, GAC and GAD) that describes the time variations of the gravity potential at satellite altitudes that are caused by non-tidal mass variability in the atmosphere and oceans^{49–51}. The GAA product describes the monthly non-tidal atmospheric mass anomalies simulated by the operational run of the atmosphere model ECMWF (European Centre for Medium-Range Weather Forecasts)⁵², GAB refers to monthly non-tidal oceanic mass anomalies simulated by the operational run of the (unconstrained) ocean model OMCT (Ocean Model for Circulation and Tides)⁵³ (for RL05) or MPIOM (Max-Planck-Institute for Meteorology Ocean Model)⁵⁴ (for RL06), GAC is the sum of GAA and GAB, and GAD can be regarded as a revised version of GAC with non-tidal atmospheric and oceanic mass anomalies only over ocean areas. GSM is just the gravity residual after GAA and GAB are removed from the GRACE observations (in other words, GSM + GAB + GAA is what GRACE satellites really measure). Consistent with this system, the LDCmgm90 data set also contains five subsets GAA, GAB, GAC, GAD and GSM, all with degree and order up to 90 because higher harmonics are not guaranteed by GRACE's measurement resolution.

The general procedures to produce the LDCmgm90 are described in Fig. 1, which is explained next.

Step 1: Obtain the LDCmgm degree-2 zonal and tesseral potential coefficients. We first obtained elements of the inertia tensor ($\Delta I_{xz}(t)$, $\Delta I_{yz}(t)$, $\Delta I_{zz}(t)$) through the mass-redistribution-related (or mass-term) angular momenta LDCgam:

$$\mathbf{h}^{\text{LDC}} \equiv (h_x^{\text{LDC}}, h_y^{\text{LDC}}, h_z^{\text{LDC}}) = \Omega (\Delta I_{xz}^{\text{LDC}}(t), \Delta I_{yz}^{\text{LDC}}(t), \Delta I_{zz}^{\text{LDC}}(t)), \quad (1)$$

then the corresponding LDCmgm degree-2 zonal and tesseral potential coefficients^{31,52}

$$\begin{aligned} \Delta C_{20}^{\text{LDC}}(t) &= \frac{1}{2\sqrt{5}} \frac{1+k'_2}{Ma^2} [\Delta T - 3\Delta I_{zz}^{\text{LDC}}(t)], \\ \Delta C_{21}^{\text{LDC}}(t) &= -\sqrt{\frac{3}{5}} \frac{1+k'_2}{Ma^2} \Delta I_{xz}^{\text{LDC}}(t), \\ \Delta S_{21}^{\text{LDC}}(t) &= -\sqrt{\frac{3}{5}} \frac{1+k'_2}{Ma^2} \Delta I_{yz}^{\text{LDC}}(t). \end{aligned} \quad (2)$$

In Eqs (1) and (2), $\Omega = 7.292115 \times 10^{-5}$ rad/s is the mean spin rate of the Earth, $k' = -0.316$ is the degree-2 load Love number³³, $M = 5.97236 \times 10^{24}$ kg and $a = 6378136.6$ m are the mass and mean equatorial radius of the Earth^{55,56}, respectively, ΔT is the change in the trace of the inertia tensor and equals zero in the current case that the global mass is conserved^{33,57}.

The LDCgam provides atmospheric angular momentum (AAM), oceanic angular momentum (OAM) and hydrological angular momentum/cryospheric angular momentum (HAM/CAM), where the HAM/CAM is dominated by but not limited to changes in land water and ice, since all the non-atmospheric and non-oceanic mass redistributions are attributed to it. Therefore, we have the following links (\rightarrow means corresponding to):

Mass-term AAM \rightarrow GAA C_{20} , C_{21} and S_{21} .
 Mass-term OAM \rightarrow GAB C_{20} , C_{21} and S_{21} .
 Mass-term HAM/CAM \rightarrow GSM C_{20} , C_{21} and S_{21} .

Then we can obtain the degree-2 GAA, GAB and GSM zonal and tesseral potential coefficients for the LDCmgm90 (please refer to the top half of Fig. 1a). Noting that CSR, GFZ, JPL and TUG all used the same AOD1B products for the given data releases (RL05 or RL06), and the JPL GAA, GAB, GAC and GAD products are the most complete, we thus chose the JPL RL06 GAA, GAB, GAC and GAD products to construct the LDCmgm90.

Step 2: Convert the Mascon gridded mass redistribution to corrected Stokes coefficients. Currently, there are three Mascon solutions CSR Mascon RL05, JPL Mascon RL05 and JPL Mascon RL06, of which the original Mascon gridded data correspond to the GSM products^{29–31}. Although the RL05 and RL06

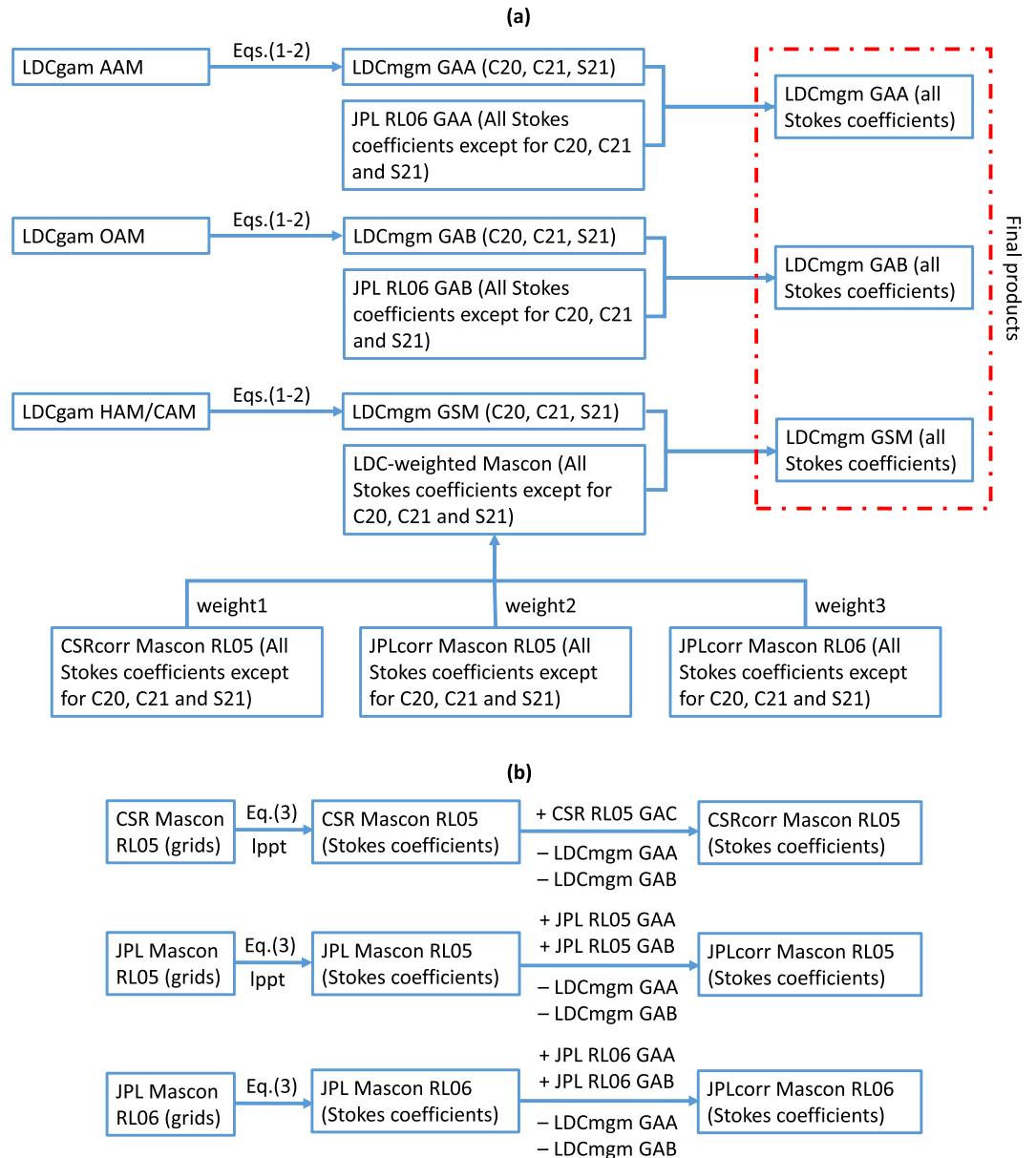


Fig. 1 Flow chart describing the procedures to generate the monthly global gravity model series LDCmgm90. **(a)** General procedures. **(b)** Procedures to obtain and correct Stokes coefficients derived from different Mascon solutions. The weights are determined by Eq. (4) and $lppt$ = long-period pole tide correction according to Wahr *et al.*²⁰.

Mascon products are based on different static background geopotential model (which would cause biases among them), we are more interested in the time-dependent parts rather than the static ones when using GRACE-like products. With these biases removed, a proper combination can extract the best components from these three Mascon solutions since no original single solution is perfect as discussed in Background & Summary.

The Mascon data are represented in the form of equivalent water height $\Delta h(\theta, \lambda, t)$ on a 0.5 degree longitude-latitude grid but representing the equal-area geodesic grid of size 1×1 degree at the equator. The surface density for this thin layer is $\Delta\sigma(\theta, \lambda, t) = \rho_w \Delta h(\theta, \lambda, t)$, where $\rho_w = 1025 \text{ kg/m}^3$ is the average density of sea water. Then the original Mascon gridded data may be converted to Stokes coefficients by⁵⁸

$$\begin{Bmatrix} \Delta C_{nm}(t) \\ \Delta S_{nm}(t) \end{Bmatrix}_{\text{surface mass}} = \frac{3}{4\pi} \frac{1 + k'_n}{\rho_{ave} (2n + 1)} \int \Delta\sigma(\theta, \lambda, t) P_{nm}(\cos\theta) \begin{Bmatrix} \cos(m\lambda) \\ \sin(m\lambda) \end{Bmatrix} \sin\theta d\theta d\lambda, \quad (3)$$

where k'_n is the degree- n load Love number (from Table 1 of Wahr *et al.*⁵⁸), $\rho_{ave} = 5517 \text{ kg/m}^3$ is the average density of the solid Earth.

The GAA RL05 produced by the ECMWF operational run contains the following two notable jumps^{49,59}:

Data	Data access
CSR GRACE RL05 GSM /GAC/GAD* ⁶¹	ftp://isdctftp.gfz-potsdam.de/grace/#
CSR GRACE RL06 GSM/GAC/GAD* ⁶²	ftp://isdctftp.gfz-potsdam.de/grace/
CSR GRACE Mascon RL05 (Version 1) ³¹	http://www2.csr.utexas.edu/grace
CSR SLR RL05 ⁶³⁻⁶⁵	ftp://ftp.csr.utexas.edu/
CSR SLR RL06 ⁶³⁻⁶⁵	ftp://ftp.csr.utexas.edu/
GFZ GRACE RL05 GSM/GAA/GAB/GAC/GAD ⁶⁶	ftp://isdctftp.gfz-potsdam.de/grace/#
GFZ GRACE RL06 GSM/GAA/GAB/GAC/GAD ⁶⁷	ftp://isdctftp.gfz-potsdam.de/grace/
JPL GRACE RL05 GSM/GAA/GAB/GAC/GAD ⁶⁸	ftp://isdctftp.gfz-potsdam.de/grace/#
JPL GRACE RL06 GSM/GAA/GAB/GAC/GAD ⁶⁹	ftp://isdctftp.gfz-potsdam.de/grace/
JPL GRACE Mascon RL05M (Version 2) ^{29,30}	http://grace.jpl.nasa.gov
JPL GRACE Mascon RL06 (Version 1) ³²	http://grace.jpl.nasa.gov
LDCgam ^{20,21,48}	https://doi.org/10.13140/RG.2.2.28698.49604
TUG ITSG-Grace2018 RL06 ¹⁴	https://doi.org/10.5880/ICGEM.2018.003

Table 1. Data used. *GAA and GAB are not provided by CSR. #No longer available since they ceased to provide the RL05 solutions very recently.

X	std ($C_{20}^X - C_{20}^{LDC}$)	std ($C_{21}^X - C_{21}^{LDC}$)	std ($S_{21}^X - S_{21}^{LDC}$)
CSR RL05 Mascon	9.456	7.121	2.981
JPL RL05 Mascon	9.626	5.471	4.903
JPL RL06 Mascon	9.950	2.588	3.602
CSR RL05	16.859	6.231	2.497
GFZ RL05	49.399	3.756	3.606
JPL RL05	15.078	5.520	3.971
CSR RL06	11.134	3.429	3.021
GFZ RL06	23.359	3.637	5.121
ITSG RL06	14.911	3.378	3.047
JPL RL06	11.222	3.054	2.934
SLR RL05	5.518	5.700	2.655
SLR RL06	5.250	3.190	2.536

Table 2. Statistical information for original GSM data (unit: 10^{-11}).

X	std ($C_{20}^X - C_{20}^{LDC}$)	std ($C_{21}^X - C_{21}^{LDC}$)	std ($S_{21}^X - S_{21}^{LDC}$)	Relative weight
CSR RL05 Mascon	7.908	6.568	5.053	0.2938
JPL RL05 Mascon	8.051	5.102	6.404	0.2924
JPL RL06 Mascon	8.222	3.003	4.068	0.4138

Table 3. Statistical information (unit: 10^{-11}) and relative weights for corrected Mascon GSM data.

- (1) Between 2006-01-29 18 h and 2006-01-30 00 h
- (2) Between 2010-01-26 00 h and 2010-01-26 06 h

due to upgrades of the horizontal and vertical resolutions in the ECMWF model, which will lead to opposite jumps in all the corresponding RL05 versions of GSM and Mascon products. Moreover, the RL05 products adopted the non-linear IERS2010 mean pole correction⁵⁶, which will cause a long-period pole tide in C_{21} and S_{21} and should be corrected as suggested by Wahr *et al.*²⁰. For the two RL05 Mascon products, corrections of the jumps and long-period pole tide should be applied (see Fig. 1b) while the RL06 data are free of these flaws due to a homogeneous reanalysis of the ECMWF data and the adoption of a linear mean pole model. However, one must keep in mind that whichever RL05 or RL06, GAA and GAB are respectively derived from the ECMWF and OMCT (or MPIOM) operational outputs, which need further refinements as shown in detailed analyses by Chen *et al.*^{21,47} and Yu *et al.*²². Thus it would be better to replace them with the LDC-corrected GAA and GAB. Further, $GAC = GAA + GAB$, and GAD can also be obtained by applying an ocean mask to GAC.

By using Eq. (3) and applying the above-mentioned corrections and replacements, we can obtain the corrected Mascon Stokes coefficients as shown in Fig. 1b.

Step 3: Take weighted average of the corrected Mascon Stokes coefficients and obtain the final solutions. The GRACE-observed geopotential V_{obs} may be separated into two parts: the part V_{obs}^{21} including

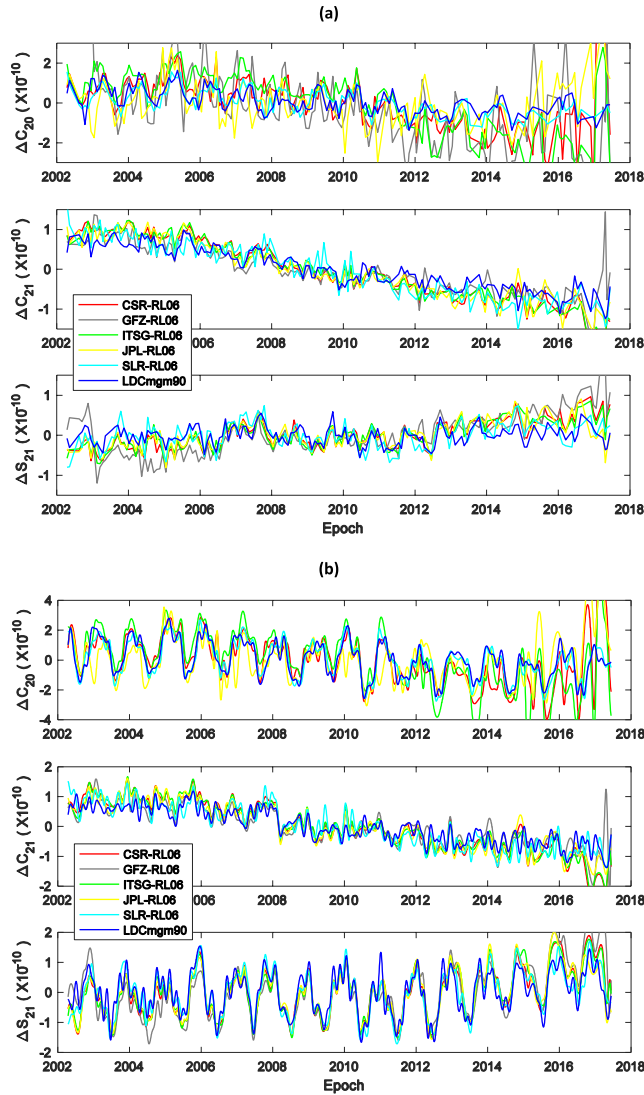


Fig. 2 C_{20} , C_{21} and S_{21} series from different sources. (a) GSM data for 163 months (no interpolation applied); (b) GSM + GAA + GAB data with cubic spline interpolations for better displays of seasonal cycles. The means of all series are removed.

the degree-2 zonal and tesseral terms (namely the terms relevant with C_{20} , C_{21} and S_{21}), and the other V_{obs}^{nzt} containing all other terms, namely $V_{obs} = V_{obs}^{zt} + V_{obs}^{nzt}$. All the CSR, GFZ, JPL and TUG released GRACE data are from the same twin satellites, thus in principle, any overestimate or underestimate of V_{obs}^{zt} will cause an opposite effect on V_{obs}^{nzt} . That is, V_{obs}^{zt} and V_{obs}^{nzt} must have the same errors for each given version of GRACE data. Based on this reasoning, the weights of the corrected Mascon Stokes coefficients may be estimated as

$$\begin{aligned}
 1/\text{weight } 1 &= \text{std}^2(C_{20}^{\text{CSRcorr05}} - C_{20}^{\text{LDCmgm}}) + \text{std}^2(C_{21}^{\text{CSRcorr05}} - C_{21}^{\text{LDCmgm}}) \\
 &\quad + \text{std}^2(S_{21}^{\text{CSRcorr05}} - S_{21}^{\text{LDCmgm}}) \\
 1/\text{weight } 2 &= \text{std}^2(C_{20}^{\text{JPLcorr05}} - C_{20}^{\text{LDCmgm}}) + \text{std}^2(C_{21}^{\text{JPLcorr05}} - C_{21}^{\text{LDCmgm}}) \\
 &\quad + \text{std}^2(S_{21}^{\text{JPLcorr05}} - S_{21}^{\text{LDCmgm}}) \\
 1/\text{weight } 3 &= \text{std}^2(C_{20}^{\text{JPLcorr06}} - C_{20}^{\text{LDCmgm}}) + \text{std}^2(C_{21}^{\text{JPLcorr06}} - C_{21}^{\text{LDCmgm}}) \\
 &\quad + \text{std}^2(S_{21}^{\text{JPLcorr06}} - S_{21}^{\text{LDCmgm}})
 \end{aligned} \tag{4}$$

since C_{20} , C_{21} and S_{21} obtained from LDCgam are the most accurate and may be approximately used as standards to infer errors in other data sets. In Eq. (4), $\text{std}(x)$ means standard derivation of x . The corresponding relative weights of the three Mascon solutions can be found in Table 3b.

We can obtain the weighted average of the corrected Mascon Stokes coefficients except for C_{20} , C_{21} and S_{21} as described in the bottom part of Fig. 1b.

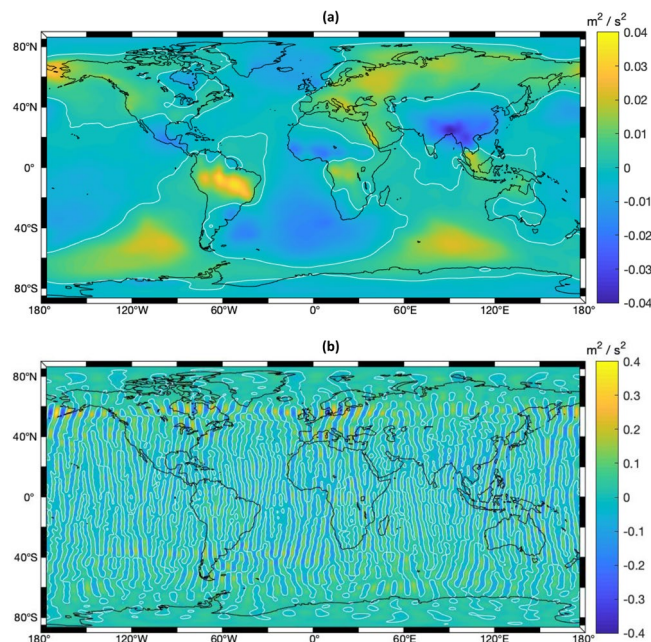


Fig. 3 Differences between the geopotential maps for Nov 2010 and Oct 2010. (a) Results from LDCmgm90; (b) Results from CSR RL06. Neither smoothing nor destriping is applied to either figure.

Data Records

Availabilities of the data used in this study are summarized in Table 1. While most GRACE and SLR data sets are named after their releasing institutes, the latest GRACE data set computed at TUG is termed ITSG-Grace2018 (ITSG for short). Data after Aug. 2016 (7 data points in total) are not provided by all RL06 GRACE products, and are supplemented by the corresponding RL05 ones.

The LDCmgm90 dataset is provided in the netcdf 4.0 format and can be accessed via figshare⁶⁰, which contains five subsets GAA, GAB, GAC, GAD and GSM, all in the form of Stokes coefficients complete from degree and order 2 to 90.

Technical Validation

The degree-2 GSM zonal and tesseral Stokes coefficients from LDCmgm90 and other individual releases are compared in Fig. 2a, while the GSM + GAA + GAB ones are compared in Fig. 2b. One can see the coefficients from LDCmgm are less noisy and free of anomalous signals presented in some other GRACE products, since when combining or assimilating data from different sources, the LDC method can provide a good handle of both the magnitude and phase aspects simultaneously for arbitrary frequency including the lowest frequency component which is usually called the trend of a series^{21,47}. The standard derivations of the original and corrected LDCmgm GSM (C_{20} , C_{21} , S_{21}) with respect with those from other model sets are provided in Tables 2 and 3, respectively. In addition, Figs 1, 3, 4 and Table 4 of Chen *et al.*²¹ implied that our C_{21} and S_{21} (the corresponding geophysical excitations are denoted as LDCgsc) are the most consistent with the observed polar motion, while Fig. 9 and Table 5 of Yu *et al.*²² suggested our C_{20} agrees the best with the observed length-of-day variations. A further and more independent check of the LDCmgm90 would be to compute the loads from the monthly gravity fields and apply those to GPS time series. However, the complexity of such a check makes it impossible to include in this short data descriptor so that will left for later work.

The mutual differences of geopotential maps for two neighboring months are also compared in Fig. 3. One can see the one corresponding to LDCmgm90 has no stripes, thanks to the Mason solutions used, while those for CSR, GFZ, JPL and TUG (only the map for CSR RL06 is provided here) have strong stripe-pattern noises, which overwhelm any geophysical signal of interest.

Code availability

The MatLab codes used to generate the LDCmgm90 are available upon request to W. Chen (wchen@sgg.whu.edu.cn).

Received: 22 March 2019; Accepted: 10 September 2019;

Published online: 23 October 2019

References

1. Tapley, B. D., Chambers, D. P., Bettadpur, S. & Ries, J. C. Large scale ocean circulation from the GRACE GGM01 Geoid. *Geophys. Res. Lett.* **30**, 2163–2166 (2002).
2. Xing, W. *et al.* Estimating monthly evapotranspiration by assimilating remotely sensed water storage data into the extended Budyko framework across different climatic regions. *J. Hydro.* **567**, 684–695 (2018).

3. Rahimi, A., Li, J., Naeeni, M. R., Shahrivand, M. & Fatolazadeh, F. On the extraction of co-seismic signal for the Kuril Island earthquakes using GRACE observations. *Geophys. J. Int.* **215**, 346–362 (2018).
4. Poropat, L. *et al.* Time variations in ocean bottom pressure from a few hours to many years: *in situ* data, numerical models, and GRACE satellite gravimetry. *J. Geophys. Res. Oceans* **123**, 5612–5623 (2018).
5. Ran, J. J. *et al.* Seasonal mass variations show timing and magnitude of meltwater storage in the Greenland Ice Sheet. *Cryosphere* **12**, 2981–2999 (2018).
6. Feng, W. & Zhong, M. Global sea level variations from altimetry, GRACE and Argo data over 2005–2014. *Geod. Geodyn.* **6**, 274–279 (2015).
7. Chambers, D. P. Observing seasonal steric sea level variations with GRACE and satellite altimetry. *J. Geophys. Res.* **111**, C03010 (2006).
8. Bettadpur, S. UTCSR level-2 processing standards document for level-2 product release 0005. Report No. GRACE 327–742 (Center for Space Research, 2012).
9. Bettadpur, S. UTCSR level-2 processing standards document for level-2 product release 0006. Report No. GRACE 327–742 (Center for Space Research, 2018).
10. Dahle, C. *et al.* GFZ GRACE level-2 processing standards document for level-2 product release 0005. Report No. STR12/02-data (Deutsches Geo Forschungs Zentrum, 2012).
11. Dahle, C. *et al.* GFZ level-2 processing standards document for level-2 product release 0006. Report No. STR18/04-data (Deutsches Geo Forschungs Zentrum, 2018).
12. Watkins, M. M. & Yuan, D. JPL level-2 processing standards document for level-2 product release 05.1. Report No. GRACE 327–744 (Jet Propulsion Laboratory, 2014).
13. Yuan, D. JPL level-2 processing standards document for level-2 product release 06. Report No. GRACE 327–744 (Jet Propulsion Laboratory, 2018).
14. Mayer-Gürr, T. *et al.* ITSG-Grace 2018-monthly, daily and static gravity field solutions from GRACE, <https://doi.org/10.5880/ICGEM.2018.003> (2018).
15. Schrama, E. J. O., Wouters, B. & Lavallée, D. A. Signal and noise in gravity recovery and climate experiment (GRACE) observed surface mass variations. *J. Geophys. Res.* **112**, B08407 (2007).
16. Swenson, S. & Wahr, J. Post-processing removal of correlated errors in GRACE data. *Geophys. Res. Lett.* **33**, L08402 (2006).
17. Wouters, B. & Schrama, E. J. O. Improved accuracy of GRACE gravity solutions through empirical orthogonal function filtering of spherical harmonics. *Geophys. Res. Lett.* **34**, L23711 (2007).
18. Duan, X. J., Guo, J. Y., Shum, C. K. & van der Wal, W. On the postprocessing removal of correlated errors in GRACE temporal gravity field solutions. *J. Geod.* **83**, 1095–1106 (2009).
19. Seo, K. W., Wilson, C. R., Han, S. C. & Waliser, D. E. Gravity Recovery and Climate Experiment (GRACE) alias error from ocean tides. *J. Geophys. Res.* **113**, B03405 (2008).
20. Wahr, J., Nerem, R. S. & Bettadpur, S. V. The pole tide and its effect on GRACE time-variable gravity measurements: Implications for estimates of surface mass variations. *J. Geophys. Res. Solid Earth* **120**, 4597–4615 (2015).
21. Chen, W., Li, J., Ray, J. & Cheng, M. Improved geophysical excitations constrained by polar motion observations and GRACE/SLR time-dependent gravity. *Geod. Geodyn.* **8**, 377–388 (2017).
22. Yu, N., Li, J. C., Ray, J. & Chen, W. Improved geophysical excitation of length-of-day constrained by Earth orientation parameters and satellite gravimetry products. *Geophys. J. Int.* **214**, 1633–1651 (2018).
23. Chen, J. L., Wilson, C. R. & Seo, K. W. Optimized smoothing of gravity recovery and climate experiment (GRACE) time-variable gravity observations. *J. Geophys. Res.* **111**, B06408 (2006).
24. Davis, J. L., Tamisie, M. E., Elósegui, P., Mitrovica, J. X. & Hill, E. M. A statistical filtering approach for Gravity Recovery and Climate Experiment (GRACE) gravity data. *J. Geophys. Res.* **113**, B04410 (2008).
25. Guo, J. Y., Duan, X. J. & Shum, C. K. Non-isotropic Gaussian smoothing and leakage reduction for determining mass changes over land and ocean using GRACE data. *Geophys. J. Int.* **181**, 290–302 (2010).
26. Han, S. C. *et al.* Non-isotropic filtering of GRACE temporal gravity for geophysical signal enhancement. *Geophys. J. Int.* **163**, 18–25 (2005).
27. Klees, R. *et al.* The design of an optimal filter for monthly GRACE gravity models. *Geophys. J. Int.* **175**, 417–432 (2008).
28. Kusche, J. Approximate decorrelation and non-isotropic smoothing of time-variable GRACE-type gravity field models. *J. Geod.* **81**, 733–749 (2007).
29. Watkins, M. M., Wiese, D. N., Yuan, D.-N., Boening, C. & Landerer, F. W. Improved methods for observing Earth's time variable mass distribution with GRACE using spherical cap mascons. *J. Geophys. Res. Solid Earth* **120**, 2648–2671 (2015).
30. Wiese, D. N., Landerer, F. W. & Watkins, M. M. Quantifying and reducing leakage errors in the JPL RL05M GRACE mascon solution. *Water Resour. Res.* **52**, 7490–7502 (2016).
31. Save, H., Bettadpur, S. & Tapley, B. D. High resolution CSR GRACE RL05 mascons. *J. Geophys. Res. Solid Earth* **121**, 7547–7569 (2016).
32. Wiese, D. N., Yuan, D.-N., Boening, C., Landerer, F. W. & Watkins, M. M. JPL GRACE mascon ocean, ice, and hydrology equivalent water height release 06 coastal resolution improvement (CRI) filtered version 1.0, <https://doi.org/10.5067/TEMSC-3MJC6> (2018).
33. Gross, R. S. Earth rotation variations – long period. In *Treatise on Geophysics 2nd edn Vol. 3* (ed. Schubert, G.) Ch. 9 (Elsevier B. V., 2015).
34. Chen, W., Ray, J., Li, J. C., Huang, C. L. & Shen, W. B. Polar motion excitations for an Earth model with frequency-dependent responses: 1. A refined theory with insight into the Earth's rheology and core-mantle coupling. *J. Geophys. Res. Solid Earth* **118**, 4975–4994 (2013).
35. Nastula, J., Ponte, R. M. & Salstein, D. A. Comparison of polar motion excitation series derived from GRACE and from analyses of geophysical fluids. *Geophys. Res. Lett.* **34**, L11306 (2007).
36. Chen, J. L. & Wilson, C. R. Low degree gravity changes from GRACE, Earth rotation, geophysical models, and satellite laser ranging. *J. Geophys. Res.* **113**, B06402 (2008).
37. Fernández, L. Analysis of geophysical variations of the C_{20} coefficient of the geopotential. In *International Association of Geodesy Symposia Vol. 133* (ed. Sideris, M.G.) (Springer, 2009).
38. Brzeziński, A., Nastula, J. & Kołaczek, B. Seasonal excitation of polar motion estimated from recent geophysical models and observations. *J. Geodyn.* **48**, 235–240 (2009).
39. Seoane, L., Nastula, J., Bizouard, C. & Gambis, D. The use of gravimetric data from GRACE mission in the understanding of polar motion variations. *Geophys. J. Int.* **178**, 614–622 (2009).
40. Jin, S., Chambers, D. P. & Tapley, B. D. Hydrological and oceanic effects on polar motion from GRACE and models. *J. Geophys. Res.* **115**, B02403 (2010).
41. Jin, S., Zhang, L. J. & Tapley, B. D. The understanding of length-of-day variations from satellite gravity and laser ranging measurements. *Geophys. J. Int.* **184**, 651–660 (2011).
42. Seoane, L., Biancale, R. & Gambis, D. Agreement between Earth's rotation and mass displacement as detected by GRACE. *J. Geodyn.* **62**, 49–55 (2012).

43. Yan, H. & Chao, B. F. Effect of global mass conservation among geophysical fluids on the seasonal length of day variation. *J. Geophys. Res.* **117**, B02401 (2012).
44. Meyrath, T. & van Dam, T. A comparison of interannual hydrological polar motion excitation from GRACE and geodetic observations. *J. Geod.* **99**, 1–9 (2016).
45. Göttl, F., Schmidt, M. & Seitz, F. Mass-related excitation of polar motion: an assessment of the new RL06 GRACE gravity field models. *Earth, Planets and Space* **70**, 195 (2018).
46. Göttl, F., Schmidt, M., Seitz, F. & Bloßfeld, M. Separation of atmospheric, oceanic and hydrological polar motion excitation mechanisms based on a combination of geometric and gravimetric space observations. *J. Geod.* **89**, 377–390 (2015).
47. Chen, W., Ray, J., Shen, W. & Huang, C. Polar motion excitations for an Earth model with frequency-dependent responses: 2. Numerical tests of the meteorological excitations. *J. Geophys. Res.: Solid Earth* **118**, 4995–5007 (2013).
48. Chen, W., Luo, J., Ray, J., Yu, N. & Li, J. C. LDCgam global angular momenta for surficial geophysical fluids, <https://doi.org/10.13140/RG.2.2.28698.49604> (2019)
49. Flechtner, F., Dobsław, H. & Fagiolini, E. Gravity Recovery and Climate Experiment: AOD1B product description document for product release 05, Report No. GRACE327-750 (Deutsches GeoForschungsZentrum, 2014).
50. Dobsław, H. *et al.* Simulating high-frequency atmosphere-ocean mass variability for dealiasing of satellite gravity observations: AOD1B RL05. *J. Geophys. Res. Oceans* **118**, 3704–3711 (2013).
51. Dobsław, H. *et al.* A new high-resolution model of non-tidal atmosphere and ocean mass variability for de-aliasing of satellite gravity observations: AOD1B RL06. *Geophys. J. Int.* **211**, 263–269 (2017).
52. Persson, A. & Grazzini, F. User guide to ECMWF forecast products, Report No. Meteorological Bulletin M3.2. (Deutsches GeoForschungsZentrum, 2007).
53. Thomas, M. Ocean induced variations of Earth's rotation – Results from a simultaneous model of global circulation and tides, PhD thesis, 129 pp., Univ. of Hamburg, Hamburg, Germany (2002).
54. Jungclauss, J. H. *et al.* Characteristics of the ocean simulations in the Max Planck Institute Ocean Model (MPIOM) the ocean component of the MPI-Earth system model. *J. Adv. Model Earth Syst.* **5**(2), 422–446 (2013).
55. Chen, W., Li, J. C., Ray, J., Shen, W. & Huang, C. L. Consistent estimates of the dynamical figure parameters of the Earth. *J. Geod.* **89**, 179–188 (2015).
56. Petit, G. & Luzum, B. (eds) IERS conventions (2010), IERS Technical Notes 36, Frankfurt am Main: Verlag des Bundesamts für Kartographie und Geodäsie, 179 pp., ISBN 3-89888-989-6 (2010).
57. Rochester, M. G. & Smylie, D. E. On changes in the trace of the Earth's inertia tensor. *J. Geophys. Res.* **79**, 4948–4951 (1974).
58. Wahr, J., Molenaar, M. & Bryan, F. Time variability of the Earth's gravity field: Hydrological and oceanic effects and their possible detection using GRACE. *J. Geophys. Res.* **103**, 30205–30229 (1998).
59. Fagiolini, E., Flechtner, F., Horwath, M. & Dobsław, H. Correction of inconsistencies in ECMWF's operational analysis data during de-aliasing of GRACE gravity models. *Geophys. J. Int.* **202**, 2150–2158 (2015).
60. Chen, W., Luo, J., Ray, J., Yu, N. & Li, J. C. LDCmgm90 monthly geopotential model set. *figshare*. <https://doi.org/10.6084/m9.figshare.7874384.v1> (2019).
61. CSR GRACE level-2 RL05 solutions, <ftp://isdcftp.gfz-potsdam.de/grace/> (2018).
62. CSR GRACE level-2 RL06 solutions, <ftp://isdcftp.gfz-potsdam.de/grace/> (2019).
63. Cheng, M. & Tapley, B. D. Variations in the Earth's oblateness during the past 28 years. *J. Geophys. Res.* **109**, B09402 (2004).
64. Cheng, M., Ries, J. C. & Tapley, B. D. Variations of the Earth's figure axis from satellite laser ranging and GRACE. *J. Geophys. Res.* **116**, B01409 (2011).
65. Cheng, M., Tapley, B. D. & Ries, J. C. Deceleration in the Earth's oblateness. *J. Geophys. Res. Solid Earth* **118**, 740–747 (2013).
66. GFZ GRACE level-2 RL05 solutions, <ftp://isdcftp.gfz-potsdam.de/grace/> (2018).
67. GFZ GRACE level-2 RL06 solutions, <ftp://isdcftp.gfz-potsdam.de/grace/> (2019).
68. JPL GRACE level-2 RL05 solutions, <ftp://isdcftp.gfz-potsdam.de/grace/> (2018).
69. JPL GRACE level-2 RL06 solutions, <ftp://isdcftp.gfz-potsdam.de/grace/> (2019).

Acknowledgements

The editorial board member Dr. Kurt Kjær and two reviewers are highly appreciated for their insightful comments and suggestions, which helped to improve this study. We also thank the CSR, GFZ, JPL and TUG GRACE/SLR teams for making the GRACE/SLR monthly solutions publicly available. The CSR GRACE mascon solutions were downloaded from <http://www2.csr.utexas.edu/grace>, while the JPL mascon data are available at <http://grace.jpl.nasa.gov>, supported by the NASA MEASUREs Program. This study is supported in parts by the National Natural Science Foundation of China (Nos 41874025 and 41474022), and the Fundamental Research Funds for the Central Universities of China (No. 2042016kf0146).

Author contributions

W. Chen designed the framework of this study and performed part of the numerical computations. J. Luo and N. Yu processed the data and also contributed to numerical computations. J. Ray and J. Li helped to refine the research framework.

Competing interests

The authors declare no competing interests.

Additional information

Correspondence and requests for materials should be addressed to W.C.

Reprints and permissions information is available at www.nature.com/reprints.

Publisher's note Springer Nature remains neutral with regard to jurisdictional claims in published maps and institutional affiliations.



Open Access This article is licensed under a Creative Commons Attribution 4.0 International License, which permits use, sharing, adaptation, distribution and reproduction in any medium or format, as long as you give appropriate credit to the original author(s) and the source, provide a link to the Creative Commons license, and indicate if changes were made. The images or other third party material in this article are included in the article's Creative Commons license, unless indicated otherwise in a credit line to the material. If material is not included in the article's Creative Commons license and your intended use is not permitted by statutory regulation or exceeds the permitted use, you will need to obtain permission directly from the copyright holder. To view a copy of this license, visit <http://creativecommons.org/licenses/by/4.0/>.

The Creative Commons Public Domain Dedication waiver <http://creativecommons.org/publicdomain/zero/1.0/> applies to the metadata files associated with this article.

© The Author(s) 2019